Enhanced FBLMS algorithm for ECG and noise removal from semg signals

Conference Paper · July 2013

DOI: 10.1109/ICDSP.2013.6622795

CITATIONS
4

READS
148

3 authors:

Mohamed El Fares Djellatou
Université du Québec à Trois-Rivières (University of Quebec At Trois Rivieres)
5 PUBLICATIONS **5** CITATIONS
SEE PROFILE

François Nougarou
Université du Québec à Trois-Rivières
46 PUBLICATIONS **233** CITATIONS
SEE PROFILE

Daniel Massicotte
Université du Québec à Trois-Rivières
162 PUBLICATIONS **999** CITATIONS
SEE PROFILE

ENHANCED FBLMS ALGORITHM FOR ECG AND NOISE REMOVAL FROM SEMG SIGNALS

Mohamed El Fares Djellatou, François Nougarou, and Daniel Massicotte

Université du Québec à Trois-Rivières, Electrical and Computer Engineering Department
C.P. 500, Trois-Rivières, Québec, Canada, G9A 5H7, Laboratory of signals and systems integration (LSSI)
{Mohamed.El.Fares.Djellatou, Francois.Nougarou, Daniel.Massicotte}@uqtr.ca}

***Abstract*— In this paper, we proposed a Dual-adapted Fast Block Least Mean Squares algorithm (DA-FBLMS) to remove electrocardiogram (ECG) and noise contaminations from surface electromyography signals (sEMG). Based on an adaptive noise cancelation (ANC) structure and artificial input signals, the ANC integrated proposed algorithm distinguishes itself by the use of an iterative method characterized by a varying number of updates for every different input block, combined with an adaptive step size guided by a QRS detector and the average error of the corresponding input block. The simulations demonstrate that the proposed DA-FBLMS algorithm presents better performances during the contaminations cancellation compared to a recursive least squares algorithm (RLS) and classic FBLMS algorithm, especially in noisy and high distortion environments.**

Keywords— Frequency domain update; adaptive block's number of updates; adaptive step size; DA-FBLMS algorithm; ECG cancellation; Adaptive noise cancellation; EMG filtering.

I. INTRODUCTION

Surface electromyography is a non-invasive and effective method of studying neuromuscular diseases, muscle fatigue, enhancement of muscular function and also human-computer interface. However, sEMG from respiratory muscles was the perfect candidate in our research due to the clear contamination by the electrocardiographic signal (ECG).

Many methods have been studied in the past 3 decades to take off the ECG contamination. The simplest ways are to implement high-pass filtering using Butterworth analog filter [1] or the gating method [2]. However, due to the frequency and time overlapping between ECG and sEMG signals, important portions of sEMG can be lost. More effective methods have been proposed like techniques based on independent component analysis (ICA) [3] or adaptive noise cancellers (ANC) on which we focus in this project.

Indeed, ANC structure is an effective method to separate an interfering signal from a signal of interest when both signals have overlapping spectra [4, 5, 6 and 7]. This method needs a reference input either recorded from an additional channel [6, 7] or artificially constructed [8]. Many algorithms have been proposed to adapt the ANC structure for ECG contamination removing from the sEMG input signals. The RLS algorithm shows high performances but it presents a strong computational complexity [6, 7]. Contrary to RLS, the FBLMS algorithm resolves this limitation due to the block factor, and on top of that, it is characterized by a high filtering capability reflected from the filter adaptation in frequency domain and the uncorrelated input blocks data [5, 9], which make it more appropriate for high distortion environments filtering. But it is known to adapt the current filter coefficients using the previous block error [5], which can be a problem especially in the case of non-stationary input signals.

For this reason, our method proposes the filtering of the same input block data twice at least, and also propose an adaptive step-size based on the QRS detection and the absolute average block error. Which offers a powerful effect on the performance of the filtering by optimally increasing the convergence speed and reducing the steady stage error. Furthermore, we examine the influence the distortion produced at the level of the patient tissue and the external electromagnetic noise (caused by the sEMG acquisition system) on the obtained performances comparing them in the same time with both classic FBLMS and RLS results.

This paper is organized as follows: Section II deals with model and signals preparation, while Section III gives the basic concept of both the ANC structure and the enhanced FBLMS algorithm (DA-FBLMS), Section IV demonstrates the performance of the proposed algorithm, and finally Section V gives important conclusions of this research.

II. SIGNALS PREPARATION–EMG, ECG AND NOISE MODELS

A. sEMG Signal Model

The basic sEMG signal model originally proposed by [8] allows generation of simulated sEMG raw data. This generation is based on the filtering of a white noise signal with a normal distribution using a filter with the appropriate spectral transfer characteristics, which can be extracted from a real sEMG using an Auto-Regressive system according to BURG's method. Note that those real sEMG were recorded in GRAN laboratory (Chiropractic department, Université du Québec à Trois-Rivières) at a sampling frequency of 1024 Hz. Afterwards, the filter's output signal will be modulated to give our modeled signal, called $s[m]$ in Fig. 1 for $m = 1,2,\dots,M$, the respiratory muscles sEMG shape, which is based on the

periodicity of two segments, the inspiration and the expiration fragments [8], where M = 10000 is the size of all signals.

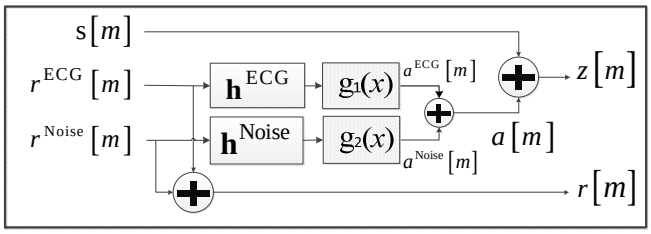

Fig. 1. The block diagram for signal Model.

B. ECG Signal Model

The ECG signal noted $r^{\mathrm{ECG}}[m]$ in Fig. 1, is constructed on the basis of the periodicity of a time interval containing just the cardiac pulses P-QRS-T of a real recorded ECG signal. The recorded interval is randomly modified for many different intervals in term of signal amplitude by the multiplication with a random noise (its values are randomly distributed between 1 and 1.2), and also in term of the interval width by adding a random number of samples for every interval, and preserving at the same time the real ECG form. The modified intervals will be concatenated to construct the ECG signal of 10000 samples. This later also gets randomly a different beat rate limited between [60, 100 beats/min] for every new simulation.

C. ECG Artifact Signal Model

In this section and according to [8], the ECG artifact, $a^{\mathrm{ECG}}[m]$ in Fig. 1, is modeled by a distorted reference ECG signal, this distortion is divided into a linear and nonlinear deformations.

The linear distortion will be carried out using a linear FIR filter, its coefficients are defined by the vector $\mathbf{h}^{\mathrm{ECG}}$, which corresponds to the tissue deformation along the propagation channel, resulting from the fact that the channels linking the heart to the recording sites are different.

In certain literature, the tissue is considered as a nonlinear channel [3], so it was required for us to add a nonlinear distortion to the output of the FIR linear filter above by calling the service of a composite nonlinear function illustrated in (1).

$$g_i(x) = \left(\frac{1}{1+\exp(-k_i\, x)} - 0.5\right)\ \gamma_i \quad \text{, with } i = 1,2 \tag{1}$$

with $g_1(\bullet)$ represent the non-linearity function which is limited between -0.5 and 0.5, x is the input signal to be distorted by the nonlinearity, k_1 is used to adjust the nonlinearity of the function. It is known from the real signals that $r^{\mathrm{ECG}}[m]$ contains more electro-cardio activity compared to $a^{\mathrm{ECG}}[m]$ because it is recorded on the chest directly above the heart, so using γ_1 as a magnitude controlling parameter is required to make sure that $a^{\mathrm{ECG}}[m]$ mean magnitude is inferior than $r^{\mathrm{ECG}}[m]$ mean magnitude to face up k_1 increasing effect on this later.

$$a^{\mathrm{ECG}}[m] = g_1\left(r^{\mathrm{ECG}}[m] * \mathbf{h}^{\mathrm{ECG}}\right) \tag{2}$$

Finally, the new ECG artifact signal is described by (2), where $*$ is the convolutional product.

D. Noise signal Model

The signals are often affected by some external noise, as an example, the electromagnetic noise released from the acquisition system. First we will model the reference noise using a random white Gaussian noise $r^{\mathrm{Noise}}[m]$, then the noise affecting the sEMG $s[m]$ is calculated in (3).

$$a^{\mathrm{Noise}}[m] = g_2\left(r^{\mathrm{Noise}}[m] * \mathbf{h}^{\mathrm{Noise}}\right) \tag{3}$$

$r^{\mathrm{Noise}}[m]$, $a^{\mathrm{Noise}}[m]$ and $\mathbf{h}^{\mathrm{Noise}}$ are respectively the reference noise, the artifact noise and coefficients of the linear deformation due to the external channel linking the recording sites (primary and reference inputs), $g_2(\bullet)$ here is the same used in (1), but with k_2 and γ_2.

III. Proposed Methods

A. ANC Technic Concept

Adaptive noise cancellation is an alternative technique of estimating and extracting a useful signal corrupted by additive interferences and noises. Its advantage lies in that with no *priori* estimates of the desired signal.

Interferences removal is facilitated when multiple sensors record the biomedical phenomenon simultaneously on different locations. The first location (primary input) and the second (reference input) should be as close as possible from the source of the noise-contaminated desired signal, and the source of the additive noise signal, $z[m]$, $r[m]$ in Fig. 2, respectively. The block diagram of "ANC" is shown in Fig. 2.

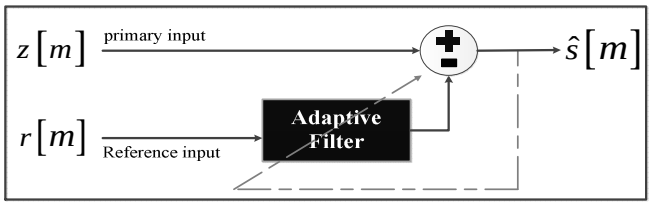

Fig. 2. The block diagram for signal Model.

The input signals in Fig. 2 are constructed in the following equations :

$$r[m] = r^{\mathrm{ECG}}[m] + r^{\mathrm{Noise}}[m] \tag{4}$$

$$a[m] = a^{\mathrm{ECG}}[m] + a^{\mathrm{Noise}}[m] \tag{5}$$

$$z[m] = a[m] + s[m] \tag{6}$$

where $r[m]$ corresponds to the reference input of the Adaptive Noise canceller, m is the sample number, a$[m]$ is the additive artifact contaminating the sEMG signal, and $z[m]$ represents the primary input to be filtered.

In the case of an ANC structure, the estimated sEMG $\hat{s}[m]$ is used to adapt the FIR filter coefficients.

B. Dual-Adapted FBLMS Algorithm (DA-FBLMS)

The algorithm used in Fig. 2 is Dual-Adapted FBLMS, which is an enhanced version of traditional FBLMS, so we will not detail just the enhancements brought. The block diagram of DA-FBLMS is shown in Fig. 3.

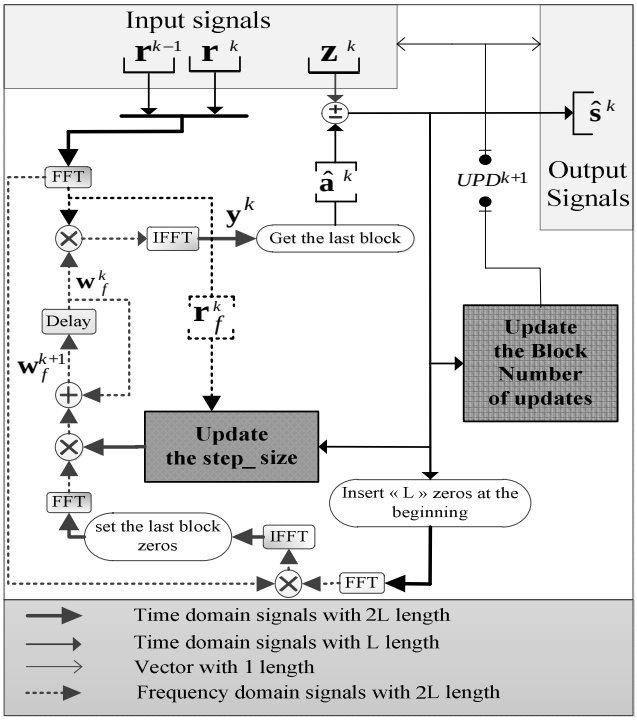

Fig. 3. The block diagram of the DA-FBLMS Algorithm .

the k^{th} block reference input (7) is a vector $\mathbf{r}^k$ defined as $\mathbf{r}^k = \{r[m]$ when $m = (1+(k-1)L),(2+(k-1)L),...,kL\}$.

$$\mathbf{r}^k = \left[r_1^k, r_2^k, r_3^k, \ldots, r_L^k\right] \tag{7}$$

L is the size of the block and k is the block number, by the same defintion above we denote the vectors $\mathbf{z}^k$, $\hat{\mathbf{s}}^k$ and $\mathbf{w}^k$ corresponding respectively to the k^{th} block primary input, the block estimate sEMG and the filter's coefficients in time domain (8) to (10).

$$\mathbf{z}^k = [z_1^k, z_2^k, z_3^k, \ldots\ldots, z_L^k] \tag{8}$$

$$\hat{\mathbf{s}}^k = [\hat{s}_1^k, \hat{s}_2^k, \hat{s}_3^k, ..., \hat{s}_L^k] \tag{9}$$

$$\mathbf{w}^k = [w_1^k, w_2^k, w_3^k, \ldots\ldots, w_L^k] \tag{10}$$

The frequency domain reference signal is noted $\mathbf{r}_f^k$ (the index f is representing the frequency domain). $\mathbf{w}_f^k$ and $\hat{\mathbf{s}}_f^k$ corresponds respectively to the frequency domain tap weights, which need to be adapted twice at least every k^{th} block iteration and the frequency domain estimated sEMG used for the adaptation of $\mathbf{w}_f^k$.

$$\mathbf{r}_f^k = \mathrm{FFT}\left(\left[\mathbf{r}^{k-1}, \mathbf{r}^k\right]\right) \tag{11}$$

$$\mathbf{w}_f^k = \mathrm{FFT}\left(\left[\mathbf{w}^k, 0_1, 0_2, ..., 0_L\right]\right) \tag{12}$$

$$\hat{\mathbf{s}}_f^k = \mathrm{FFT}\left(\left[0_1, 0_2, \ldots\ldots, 0_L, \hat{\mathbf{s}}^k\right]\right) \tag{13}$$

The estimated interferences $\hat{\mathbf{a}}^k = \left[\hat{a}_1^k, \hat{a}_2^k, \hat{a}_3^k, \ldots, \hat{a}_L^k\right]$ is the last (second) block of $\mathbf{y}^k$.

$$\mathbf{y}^k = \mathrm{IFFT}\left(\mathbf{w}_f^k \mathbf{r}_f^k\right) \tag{14}$$

$$\hat{\mathbf{a}}^k = \left[y_{L+1}^k, y_{L+2}^k, ..., y_{2L}^k\right] \tag{15}$$

The k^{th} block vector of the estimated sEMG $\hat{\mathbf{s}}^k$ is computed as :

$$\hat{\mathbf{s}}^k = \mathbf{z}^k - \hat{\mathbf{a}}^k \tag{16}$$

1) The adaptive block's number of updates:

Inspired from [10], we use the mean absolute error of the k^{th} block noted e_{av}^k calculated directly from $\hat{\mathbf{s}}^k$.

$$e_{\mathrm{av}}^k = \frac{1}{L}\sum_{n=1}^{L}\left|\hat{\mathbf{s}}^k\right| \tag{17}$$

We adapt the block's number of updates based on (18) to (24).

$$UPD^{k+1} = UPD^k / 2 \quad \text{for } e_{\mathrm{av}}^k = e_{\mathrm{av}}^{k-1} = 0 \tag{18}$$

$$\Delta F^k = \begin{cases} (1-\alpha)\dfrac{\rho_1}{e_{\mathrm{av}}^k} - \alpha\dfrac{\rho_2}{(e_{\mathrm{av}}^k - e_{\mathrm{av}}^{k-1})} & \text{for } e_{\mathrm{av}}^k > e_{\mathrm{av}}^{k-1}, e_{\mathrm{av}}^k \neq 0, e_{\mathrm{av}}^{k-1} \neq 0 \\ \alpha\dfrac{\rho_1}{e_{\mathrm{av}}^k} - (1-\alpha)\dfrac{\rho_2}{(e_{\mathrm{av}}^k - e_{\mathrm{av}}^{k-1})} & \text{for } e_{\mathrm{av}}^k \leq e_{\mathrm{av}}^{k-1}, e_{\mathrm{av}}^k \neq 0, e_{\mathrm{av}}^{k-1} \neq 0 \\ (1-\alpha)\dfrac{\rho_2}{e_{\mathrm{av}}^{k-1}} & \text{for } e_{\mathrm{av}}^k = 0, e_{\mathrm{av}}^{k-1} \neq 0 \\ (1-\alpha)\dfrac{\rho_1}{e_{\mathrm{av}}^k} & \text{otherwise} \end{cases} \tag{19}$$

where ρ_1, ρ_2 are respectively the increasing and the decreasing factor limited in the range [0, 1], α is a weighting coefficient which control the excessive effect of ρ_1, ρ_2 for providing proper values for k^{th} updates factor ΔF^k.

Afterward, if ΔF^k is superior then the threshold value Π^k, the $(k+1)^{th}$ block's number of updates UPD^{k+1} follows (18). Otherwise, it follows (20).

$$UPD^{k+1} = 2UPD^k \tag{20}$$

Furthermore; we should limit UPD^{k+1} to prevent any excessive effect, according to (21) and (22):

$$UPD^{k+1} > \mathrm{UPD}_{Max} \Rightarrow UPD^{k+1} = \mathrm{UPD}_{Max} \tag{21}$$

$$UPD^{k+1} < \mathrm{UPD}_{Min} \Rightarrow UPD^{k+1} = \mathrm{UPD}_{Min} \tag{22}$$

where UPD_{Max}, UPD_{Min} are respectively the maximum and the minimum block's number of updates defined empirically by the user. The threshold value Π^k decrease along with every new input block data as illustrated in (23).

$$\Pi^{k+1} = \Pi^k - \delta_1 \, DF_1^k \tag{23}$$

we note Π^0 the initial threshold value. DF_1^k is the threshold decreasing factor which depends on e_{av}^k and e_{av}^{k-1} (24).

$$DF_1^k = \exp(\lambda_1 (e_{\mathrm{av}}^k e_{\mathrm{av}}^{k-1})) \tag{24}$$

δ_1, λ_1 are controlling coefficients. Henceforth, we will use the term u to define the update number of every input block data (u = 1,2,…, UPD_{Min}, UPD_{Min} +1, UPD_{Min} +2,…, UPD_{Max}).

2) The adaptive step-size:

In this part we need to use two different adaptive step-sizes: (i) a bigger one for the filtering of the QRS pulses and (ii) a smaller one for the rest of $\mathbf{r}^k$. The QRS detection used was defined in the literature [3]. Both these adaptive step sizes decrease with every new update. The decreased portion $DF_2^{k,u}$ of the k^{th} block and u^{th} update changes according to $e_{\mathrm{av}}^{k,u}$ and $e_{\mathrm{av}}^{k,u-1}$ as shown in (25).

$$DF_2^{k,u} = \exp(\lambda_2 (e_{\mathrm{av}}^{k,u} e_{\mathrm{av}}^{k,u-1})) \tag{25}$$

where $e_{\mathrm{av}}^{k,u}$ is absolute average block error corresponding to the k^{th} block and the u^{th} update.

In addition, the power estimation [5] of input blocks is used to normalise the adaptive step-size according to (26).

$$\mathbf{P}^k = \beta \, \mathbf{P}^{k-1} + (1-\beta) \left(\mathbf{r}_f^k\right)^2 \tag{26}$$

β is the amnestic factor, and δ_2, λ_2 are controlling coefficients. The decreasing of the step-sizes is illustrated in Fig. 4, where μ_{QRS}, μ_{noQRS} and $\mu^{k,u+1}$ are respectively the step sizes used for updating the filter when there are QRS pulses, the step size when there are no QRS pulses in the input block data and the step size used in the next filter's coefficients update $(u+1)^{th}$. Then all the step sizes are limited between μ_{Min} and μ_{Max} defined emperically by the user. μ_{QRS}^0 is equal to μ_{Max} and superior than μ_{noQRS}^0. While *i*, *j* are respectively the number of update corresponding to QRS, no QRS filtering of input block data.

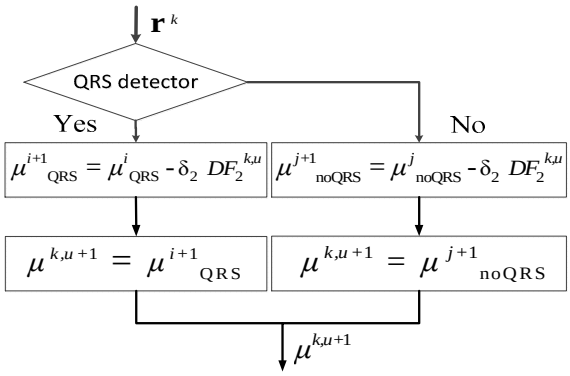

Fig. 4. The Followed algorithm to compute the adaptive step-size.

II. SIMULATION RESULTS

To evaluate the performance of the proposed adaptive DA-FBLMS, classic FBLMS and RLS algorithms; we used the confirmed outperforming parameters illustrated in TABLE. I according to some past simulations. L and μ are respectively the filter tap weights length and the step size used. λ is the forgetting factor used for RLS algorithm. The following parameters correspond to the fixed parameters for the whole process, $\beta = 0.9$, $\alpha = 0.4$, $\delta_2 = 0.1$, $\delta_2 = 0.1$, $\Pi^0 = 50$, $\rho_1 = 0.5$, $\rho_2 = 0.6$, $\lambda_1 = 500$, $\lambda_2 = 10$.

TABLE I. PARAMETER VALUES FOR STUDIED METHODS.

DA-FBLMS		RLS		FBLMS	
$2L$	256	L	64	$2L$	256
$\mu_{\max}$	0.014	μ	1.23		
$\mu_{\min}$	0.010	λ	0.999	μ	0.0115

A. Experiment 1

First, we fixed respectively $UPD_{\mathrm{Min}} / UPD_{\mathrm{Max}} = 2/4$. A comparison between the performance of DA-FBLMS (2/4), FBLMS and RLS was carried out using the metric mean coherence noted $\overline{Coh}$ as illustrated in (28), which correspond

to the mean of the coherence $Coh(f)$ between $s[m]$ and $\hat{s}[m]$.

$$Coh(f) = \frac{\left|P_{s,\hat{s}}(f)\right|^2}{P_s(f)\ P_{\hat{s}}(f)} \tag{27}$$

$$\overline{Coh} = \frac{1}{F_{\text{Max}}} \sum_{f=0}^{F_{\text{Max}}} Coh(f) \tag{28}$$

where $P_{s,\hat{s}}(f)$, $P_s(f)$, $P_{\hat{s}}(f)$ are respectively the cross-spectral density, auto-spectral densities of $s[m]$ and $\hat{s}[m]$, F_{MAX} is the maximum frequency used, which is 500 Hz in our case.

The simulations were launched using a linear and a no linear channels. Every simulation contains 100 realizations characterized by different random beat rates limited between [60, 100 beats/min], moreover the QRS amplitudes and R-R intervals change randomly every new realization.

TABLE II. DISTORTION PARAMETERS DEFINED IN SECTION II FOR A LINEAR AND A NO LINEAR ENVIRONEMENTS.

ENVIRONEMENT	ECG			Noise		
	$\mathbf{h}^{ECG}$	k_1	γ_1	$\mathbf{h}^{Noise}$	k_2	γ_2
LINEAR	$\mathbf{h}^{ECG}$	—	—	$\mathbf{h}^{Noise}$	—	—
NO - LINEAR	$\mathbf{h}^{ECG}$	5	30	$\mathbf{h}^{Noise}$	0.6	6.5

$\mathbf{h}^{ECG}$ = [0.1 -0.045 1 0.25 -0.6].

$\mathbf{h}^{Noise}$ = [0.99 0.01 0.002 0.6].

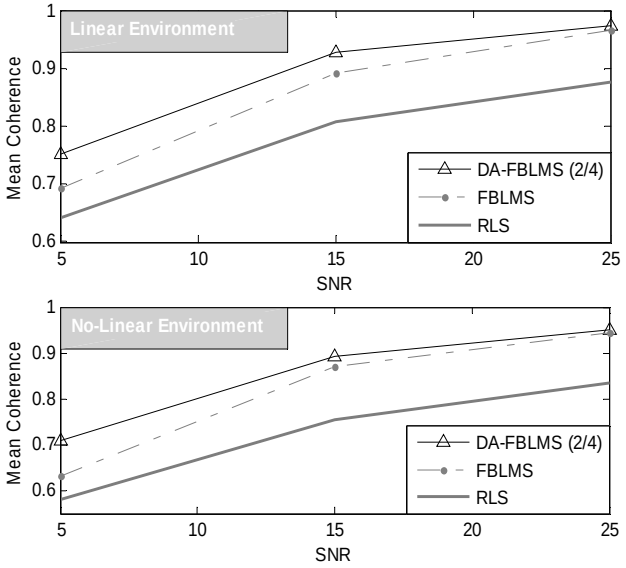

Fig. 5. Metric performance comparison based on $\overline{Coh}$ for RLS, FBLMS and proposed DA-FBLMS for different channel conditions defined by SNR of 5dB, 15dB and 25 dB.

According to Fig. 5, we observe a decrease in performances of the DA-FBLMS, classic FBLMS and RLS with any decrease of the SNR. But it shows better performances in case of DA-FBLMS compared to FBLMS in term of stability toward SNR decrease. Those results are due to the adaptation of every block twice at least according to the absolute average block error which can face up the limitation due to the fact that the FBLMS filters the current block input by the previous tap weights which means according to previous block error.

The Frequency implementation of LMS algorithm had better results compared to RLS by dint of the frequency domain updated tap weights which made easier the optimum coefficient research and more efficient.

The SNR shown in Fig. 5 and Table. III correspond to the quantity of the artifact noise $a^{\text{Noise}}[m]$ compared to the quantity of sEMG signal $s[m]$.

B. *Experiment 2*

In this experiment, we will show the effect of updating the same block many times according to the block error, on the DA-FBLMS performances for different SNRs. this later will also be compared with other algorithms like classic FBLMS and RLS.

TABLE III. THE MEAN COHERENCE (28) VERSUS SNR FOR DA-FBLMS WITH DIFFERENTS MIN /MAX NUMBER OF UPDATES, FBLMS, RLS.

ENVIRONEMENT	THE USED ALGORITHM	SNR (*dB*)		
		5	***15***	**25**
LINEAR	DA-FBLMS (2/4)	0.7506	0.9264	**0.9727**
	DA-FBLMS (2/6)	0.7589	**0.9378**	0.9694
	DA-FBLMS (2/8)	**0.7658**	0.9327	0.9634
NO - LINEAR	DA-FBLMS (2/4)	0.7090	0.8926	**0.9506**
	DA-FBLMS (2/6)	0.7167	**0.9086**	0.9463
	DA-FBLMS (2/8)	**0.7236**	0.8996	0.9408

Increasing both the minimum and the maximum number of updates improves the performance of the DA-FBLMS algorithm until a certain threshold (number of updates) where the behavior of the filtering process adopts decreasing performances. This threshold depends on the quantity of acquisition noise, as shown in Table. III. Indeed increasing the number of updates is preferable in high noise environements and not previliged in low noise environements.

The fact of filtering the input data by blocks in place of every sample (RLS or LMS case) decrease clearly the computational complexity of FBLMS, which can be given in exchange for higher performances as in the case of DA-FBLMS.

C. *Experiment 3*

Now we will see the effect of the adpative step size on the proposed algorithm ($UPD_{Min}/UPD_{Max} = 2/4$) DA-FBLMS for two fixed (big and small) step-sizes and one adaptive step size limited between these two laters as shown in Fig. 6 below,

which give the coherence distributions between [0, 50 Hz], in other words the ECG removal performances.

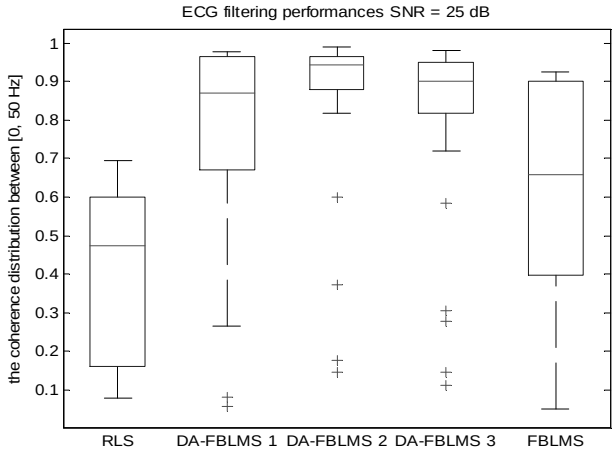

Fig. 6. The distribution of the coherence (SNR = 25 dB), for frequencies between [0, 50 Hz] for RLS, FBLMS and the proposed method DA-FBLMS with 1) $\mu_{Min}=\mu_{Max}=0.01$, 2) $0.01<\mu\leq 0.04$ *and 3)* $\mu_{Min}=\mu_{Max}=0.04$.

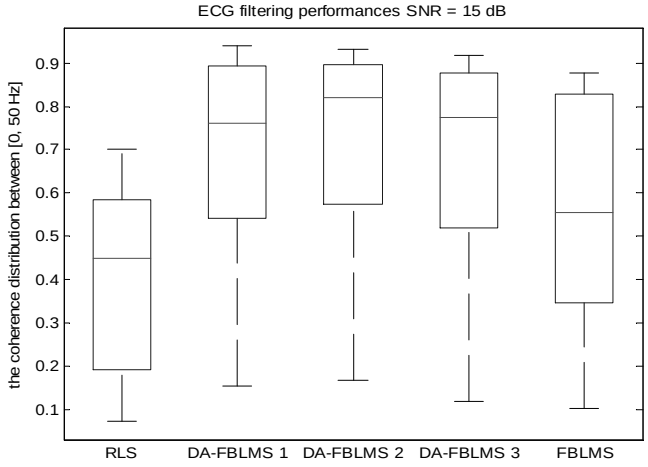

Fig. 7. The distribution of the coherence (SNR = 15 dB), for frequencies between [0, 50 Hz] for RLS, FBLMS and the proposed method DA-FBLMS with 1) $\mu_{Min}=\mu_{Max}=0.01$, 2) $0.01<\mu\leq 0.04$ *and 3)* $\mu_{Min}=\mu_{Max}=0.04$.

The results in Fig. 6 and Fig. 7 present boxplots (Matlab Command) giving the median and the distribution of the coherence (27), for the algorithms mentioned above, using a linear channel with 25 and 15 dB of SNR respectively. We can clearly notice that the adaptive size DA-FBLMS shows the highest performances for ECG filtering due to the proposed QRS detector service when adapting the step-size.

We can also certify the good filtering obtained by the proposed DA-FBLMS compared to RLS and Classic FBLMS even for fixed step sizes.

V. Conclusion

A novel adaptive step-size based on QRS detection and adaptive block's number of updates DA-FBLMS algorithm has been introduced, which showed better results in term of coherence compared to RLS and FBLMS. In addition, these results were proved for 100 different artifacts and for different external environments.

Acknowledgment

The authors wish to thank the Microsystems Strategic Alliance of Quebec and the Natural Sciences and Engineering Research Council of Canada for its financial support.

References

[1] T. Eye and H. Assessment, "High-pass filtering to remove electrocardiographic interference from torso EMG recordings," pp. 1–5, 1993.

[2] V. von Tscharner, B. Eskofier, and P. Federolf, "Removal of the electrocardiogram signal from surface EMG recordings using non-linearly scaled wavelets.," *Journal of electromyography and kinesiology : official journal of the International Society of Electrophysiological Kinesiology*, vol. 21, no. 4, pp. 683–8, Aug. 2011.

[3] J. Pan and W. J. Tompkins, "A Real-Time QRS Detection Algorithm," IEEE Trans. on Biomedical Engineering, vol. BME-32, no. 3, pp. 230–236, Mar. 1985.

[4] T. M. Jamel, "Performance Improvements of Adaptive Noise Canceller Using New Adajusted Step Size LMS Algorithm," no. Icsps, 2011.

[5] M. Z. U. Rahman, R. A. Shaik, and D. V. R. K. Reddy, "Denoising ECG Signals Using Transform Domain Adaptive Filtering Technique," 2009 Annual IEEE India Conf., vol. 0, no. 1, pp. 1–4, 2009.

[6] G. Lu, J.-S. Brittain, P. Holland, J. Yianni, A. L. Green, J. F. Stein, T. Z. Aziz, and S. Wang, "Removing ECG noise from surface EMG signals using adaptive filtering," Neuroscience Letters, vol. 462, no. 1, pp. 14–19, Sep. 2009.

[7] M. Golabbakhsh, M. Masoumzadeh, and M. F. Sabahi, "ECG and power line noise removal from respiratory EMG signal using adaptive filters," vol. 5, no. 4, pp. 28–33, 2011.

[8] Y. Deng, W. Wolf, R. Schnell, and U. Appel, "New aspects to event-synchronous cancellation of ECG interference: an application of the method in diaphragmatic EMG signals.," IEEE Trans. on bio-medical engineering, vol. 47, no. 9, pp. 1177–84, Sep. 2000.

[9] B. Rafaely and S. J. Elliot, "A computationally efficient frequency-domain LMS algorithm with constraints on the adaptive filter," IEEE Trans. on Signal Processing, vol. 48, no. 6, pp. 1649–1655, Jun. 2000.

[10] Q. Yang, L. Xiao, X. Zeng, and J. Wang, "Adaptive Step-size and Block-size FBLMS Algorithm," 2009 Int. Conf. on Computer Engineering and Technology, pp. 8–12, Jan. 2009.

[11] C. Feng, N. Tong, and Y. Yang, "A New Variable Step-Size BLMS Algorithm Based on Discrete Wavelet Transforms," 2010 Second WRI Global Congress on Intelligent Systems, pp. 285–287, Dec. 2010.

[12] B. Farhang-Boroujeny, "Analysis of the frequency-domain block LMS algorithm," IEEE Trans. on Signal Processing, vol. 48, no. 8, pp. 2332–2342, 2000.

[13] T. W. Schweitzer, J. W. Fitzgerald, J. A. Bowden, and P. Lynne-Davies, "Spectral analysis of human inspiratory diaphragmatic electromyograms.," Journal of applied physiology: respiratory, environmental and exercise physiology, vol. 46, no. 1, pp. 152–65, Jan. 1979.